RSC Advances

PAPER

View Article Online
View Journal | View Issue

Cite this: *RSC Adv.*, 2025, **15**, 41209

Degradation of oxytetracycline in wastewater by catalytic ozonation with eggshell-derived calcium peroxide

Apiradee Sukmilin, *[a] Piyapong Pankaew,[b] Jaroenporn Chokboribal[c] and Chalor Jarusutthirak[d]

Received 2nd September 2025
Accepted 9th October 2025

DOI: 10.1039/d5ra06601h

rsc.li/rsc-advances

Calcium peroxide (CaO_2) was successfully synthesized from calcium-rich eggshell waste through a multi-step process. First, the eggshell waste was naturally dried, ground, and calcined at varying temperatures (700, 800, or 900 °C) for 2 hours, resulting in the formation of calcium oxide (CaO). Subsequently, CaO_2 was synthesized *via* a precipitation method, in which CaO was mixed with hydrogen peroxide (H_2O_2) at varying concentrations (25%, 30%, or 35%). The formation of CaO_2 was initially confirmed by its characteristic yellowish appearance. The properties of the eggshell waste, CaO, and CaO_2 were characterized using X-ray diffractometry (XRD), Fourier-transform infrared spectroscopy (FTIR), and scanning electron microscopy (SEM). The XRD results indicated that higher calcination temperatures enhanced the crystallinity of CaO, while increasing the H_2O_2 concentration led to a reduction in the crystalline structure of CaO_2. The performance of CaO_2 as a catalyst in catalytic ozonation was evaluated for the degradation of oxytetracycline (OTC) in synthetic wastewater. Under the designated conditions (pH 7, 3 g per L CaO_2, and 60 min reaction time), OTC removal efficiency reached 100%, whereas sole ozonation achieved only 85.7%. The pseudo-first-order reaction rate constant (k_{obs}) for composite B (30% H_2O_2 with 1 : 1 mole ratio between CaO and H_2O_2) was 0.1152 min^{-1}, which was significantly higher than that of sole ozonation ($k_{obs} = 0.0365$ min^{-1}), demonstrating the catalytic efficiency of CaO_2.

1. Introduction

Calcium peroxide (CaO_2) has garnered increasing attention in wastewater treatment due to its versatility as an oxidant and controlled-release source of hydrogen peroxide (H_2O_2).[1] As a thermally stable inorganic peroxide, the hydrolysis of CaO_2 generates both H_2O_2 and calcium hydroxide ($Ca(OH)_2$), facilitating its application in both biological and chemical treatment processes.[2] In activated sludge processes, CaO_2 has been used as an oxygen source, enhancing microbial degradation of organic pollutants while reducing energy-intensive aeration requirements.[3] In addition, it has demonstrated high efficiency in heavy metal removal, where the combined effects of H_2O_2 oxidation and $Ca(OH)_2$ precipitation enable the removal of heavy metals (Pb, Cu, Zn, Ni, Cd, As).[4,5] Furthermore, CaO_2 plays a crucial role in advanced oxidation processes (AOPs), particularly in the degradation of recalcitrant contaminants such as dyes,[6,7] phenol,[8] and emerging contaminants,[9–11] through the generation of hydroxyl radicals ($OH^•$). Several studies have explored its application as a catalyst in the ozonation process, wherein its controlled dissolution facilitates the gradual release of H_2O_2.[7,8] This synergistic effect has been reported to improve the degradation of pharmaceutical products, such as sulfonamide,[9] metronidazole,[10] sulfamethoxazole,[11] oxytetracycline,[12] sulfolane,[13] and diclofenac,[14] achieving removal efficiencies of up to 80%. Furthermore, the alkaline conditions induced by $Ca(OH)_2$ accelerate ozone decomposition into reactive species, further enhancing pollutant degradation. Its environmentally friendly nature, cost-effectiveness, and ease of handling compared to other oxidants, make CaO_2 a promising alternative for sustainable wastewater treatment.[7,10,11]

The synthesis of CaO_2 in the presence of H_2O_2 has been studied extensively, with various calcium precursors, including calcium chloride ($CaCl_2$), calcium hydroxide ($Ca(OH)_2$), calcium nitrate ($Ca(NO_3)_2$), and calcium sulfate ($CaSO_4$).[15–17] However, the high cost and environmental concerns associated with conventional precursors have driven interest in sustainable alternatives. Eggshell waste, an abundant calcium-rich byproduct, has emerged as a promising raw material for CaO_2 synthesis due to its high calcium carbonate ($CaCO_3$) content.[18] Eggshell waste was chosen because it is abundant, cost-

---

[a] Faculty of Science and Technology, Phranakhon Rajabhat University, Bangkok 10220, Thailand. E-mail: Apiradee@pnru.ac.th

[b] Division of Industrial Materials Science, Faculty of Science and Technology, Rajamangala University of Technology Phra Nakhon, Bangkok 10800, Thailand

[c] Materials Science Program, Faculty of Science and Technology, Phranakhon Rajabhat University, Bangkok 10220, Thailand

[d] Department of Environmental Technology and Management, Faculty of Environment, Kasetsart University, Bangkok 10900, Thailand

effective, and environmentally friendly, providing a low-cost raw material while reducing waste and adding environmental and economic value. Utilizing eggshell waste as a precursor not only provides a cost-effective and environmentally friendly alternative but also aligns with circular economy principles by mitigating waste disposal issues associated with large-scale hatcheries.[18,19] The synthesis of CaO_2 from eggshell waste using precipitation typically involves a two-step process: thermal decomposition of $CaCO_3$ to calcium oxide (CaO) at temperatures exceeding 700 °C, followed by the reaction of CaO with H_2O_2 to form CaO_2.[20,21] Studies have demonstrated that complete conversion of $CaCO_3$ to CaO occurs at approximately 900 °C, underscoring the critical role of temperature in optimizing CaO formation.[20,21] Despite the potential of CaO_2 synthesis from eggshell waste, published research on the topic remains limited, particularly regarding optimizing key synthesis parameters such as calcination temperature, H_2O_2 concentration, and the $Ca(OH)_2$-to-H_2O_2 molar ratio. These factors substantially influence the properties of the synthesized CaO_2, which in turn determine its performance in environmental applications, particularly in catalytic ozonation.[22]

Among emerging contaminants in water systems, antibiotics such as oxytetracycline (OTC) pose major environmental risks due to their extensive use in aquaculture, animal husbandry, and agriculture.[23,24] Often, conventional wastewater treatment processes are insufficient for complete OTC degradation, leading to its persistence in aquatic environments and contributing to the proliferation of antibiotic resistance.[25] While ozonation is widely used for OTC removal, often its efficiency is hindered by the formation of toxic by-products.[25,26] AOPs that combine ozone (O_3) with H_2O_2 have demonstrated enhanced OTC degradation by generating $OH^{\bullet}$ radicals.[12,27] However, direct H_2O_2 addition presents challenges related to rapid decomposition and handling difficulties. As a controlled-release H_2O_2 source, CaO_2 offers a more stable and efficient alternative in catalytic ozonation.[28] Despite the promising potential of CaO_2 synthesized from eggshell waste as a catalyst in ozonation, its application in OTC degradation remains unexplored. Furthermore, no published research has systematically investigated the effects of synthesis parameters, including calcination temperature, H_2O_2 concentration, and molar ratio, on the physicochemical characteristics and catalytic efficiency of eggshell-derived CaO_2 in ozonation applications.

Thus, the current study aimed to synthesize CaO_2 from eggshell waste using a precipitation method while systematically optimizing key synthesis parameters: calcination temperature, H_2O_2 concentration, and the $Ca(OH)_2$-to-H_2O_2 molar ratio. The physicochemical properties of the synthesized CaO_2 were characterized using X-ray diffractometry (XRD) and Fourier-transform infrared spectroscopy (FTIR). Then, the catalytic efficiency of CaO_2 in ozonation was evaluated based on batch experiments using OTC as a model antibiotic. This research should contribute to the development of sustainable and efficient strategies for the treatment of OTC or other antibiotic contaminants, or both, in wastewater systems. The methodology and overview of the present study are summarized in Fig. 1.

2. Experimental

2.1. Materials

The collected eggshell waste was dried at 100 °C for 2 hours, then crushed into small pieces and stored in a desiccator before use. This experiment used analytical-grade reagents, including oxytetracycline (Thermo Fisher Scientific), hydrogen peroxide (35%, Chem-Supply), sodium hydroxide (Ajax), and sulfuric acid (RCI Labscan). Commercial calcium peroxide (30%, STP Chem Solution) was used as a reference for comparison with the synthesized calcium peroxide from the eggshell waste. Sodium thiosulfate (Kemaus) was used to quench residual ozone. All solutions were prepared using deionized water.

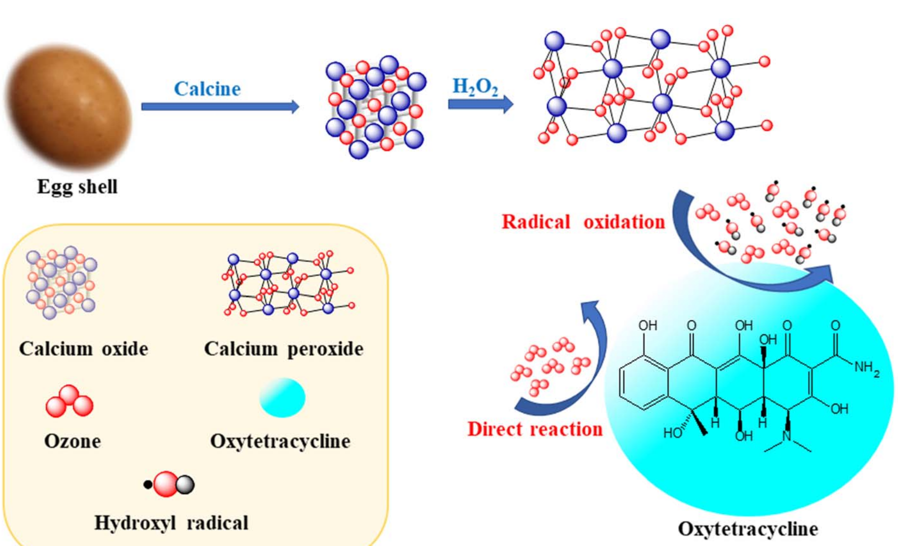

Fig. 1 Schematic summary of the methodology and results of present study.

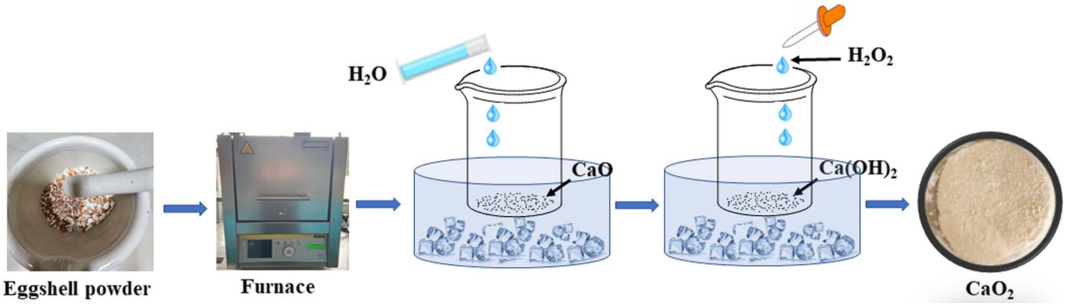

Fig. 2 Schematic diagram of calcium peroxide (CaO_2) synthesis from eggshell waste.

2.2. Preparation of CaO_2 from eggshell waste

CaO_2 was synthesized from eggshell waste using a calcination and precipitation method,[20] as shown in Fig. 2. The eggshell waste was calcined at 700 °C, 800 °C, or 900 °C for 2 hours. After calcination, the resulting CaO was added to water under an ice bath to form $Ca(OH)_2$. The concentration of H_2O_2 was varied (25%, 30%, or 35%), with different $Ca(OH)_2$-to-H_2O_2 molar ratios (1 : 1, 7 : 1, 8.5 : 1, or 10 : 1), as shown in Table 1. The formation of CaO_2 was indicated by the appearance of a yellowish slurry. The synthesized CaO_2 was characterized using XRD, FTIR, and SEM. The final product was stored in a desiccator prior to use.

2.3. Characterization of eggshell waste, CaO, and CaO_2

The eggshell waste, calcined eggshell waste, and synthesized calcium peroxide were characterized to determine their structural, chemical, and morphological properties using XRD, FTIR, and SEM, as detailed below.

2.3.1. X-ray diffraction. X-ray Diffraction (XRD) was performed to identify the crystalline phases of the samples. The XRD data were collected using a Philips X'Pert-MPD X-ray diffractometer (PW 3020 vertical goniometer and PW 3710 MPD control unit) with Bragg–Brentano para-focusing optics. The diffraction patterns were recorded in the 2θ range of 10–70° with a scanning rate of 2° min^{-1}. The phase composition of the samples was determined using the direct peak intensity comparison method.[29]

2.3.2. Fourier transformed infrared spectroscopy. Fourier-transform infrared spectroscopy (FTIR) analysis was conducted to identify the functional groups present in the samples. The spectra were recorded using a PerkinElmer FTIR spectrometer in attenuated total reflectance (ATR) mode with a resolution of 4 cm^{-1} over the wavenumber range 4000–500 cm^{-1}. Prior to analysis, the samples were dried at 100 °C overnight to remove residual moisture.

2.3.3. Scanning electron microscopy. Scanning electron microscopy (SEM) analysis was performed to examine the surface morphology and elemental composition of the samples. Images were captured using a JEOL-JSM 5600 LV microscope equipped with a 6587 energy-dispersive X-ray spectroscopy (EDS) detector at an accelerating voltage of 15 kV. The samples were mounted on a sample holder using adhesive carbon foil and sputter-coated with gold to enhance conductivity.

Table 1 H_2O_2 concentrations and $Ca(OH)_2$-to-H_2O_2 molar ratios used in CaO_2 synthesis

Composite	Concentration of H_2O_2 (%)	Molar ratio ($Ca(OH)_2 : H_2O_2$)
A	25	1 : 1
B	30	1 : 1
C	35	1 : 1
D	25	7 : 1
E	30	8.5 : 1
F	35	10 : 1

2.4. Investigation of catalytic ozonation efficiency

The catalytic ozonation experiments were conducted to evaluate the efficiency of synthesized calcium peroxide for the degradation of oxytetracycline (OTC). The ozonation system was operated at ambient temperature, with ozone generated from dry air using an ozone generator. In the catalytic ozonation process, synthesized calcium peroxide was introduced into the reactor. The initial OTC concentration was set at 5 mg L^{-1}, with a solution pH of 7 and a calcium peroxide dosage of 3 g L^{-1}. Unreacted ozone was trapped using a 2% potassium iodide solution. The residual OTC concentration was measured using a UV-Vis spectrophotometer at 272 nm. All experiments were conducted in triplicate, with the results presented as average values from three independent measurements, with results shown in figures and tables. Sole ozonation (without calcium peroxide) was performed as a control experiment under identical conditions to compare its efficiency with catalytic ozonation.

3. Results and discussion

3.1. Characterization of eggshell waste, CaO, and CaO_2

3.1.1. X-ray diffraction analysis. Eggshell waste was calcined at 700 °C, 800 °C, or 900 °C for 2 hours to investigate phase transformations using XRD. The XRD patterns of both raw and calcined eggshell waste samples are presented in Fig. 3. The XRD pattern of the raw eggshell waste had diffraction peaks at $2\theta = 29.40°$ (104), 36.0° (110), 39.42° (113), 43.2° (202), and 47.50° (116), corresponding to the crystallographic planes of

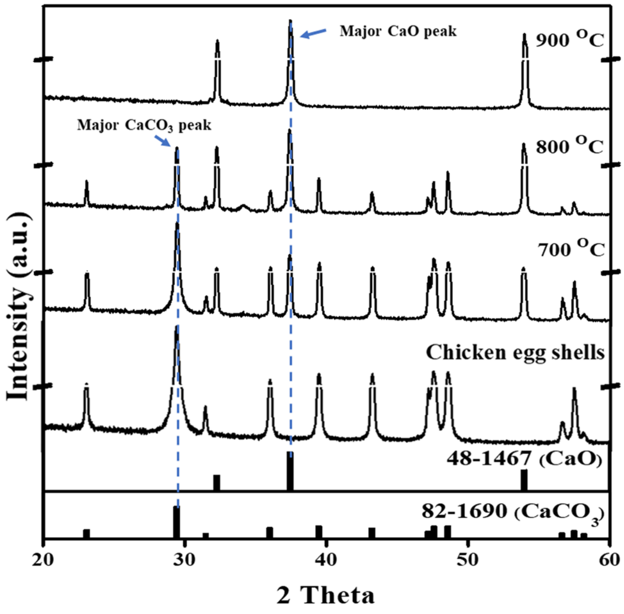

Fig. 3 XRD patterns of eggshell waste calcined at different temperatures.

calcium carbonate ($CaCO_3$) based on the Joint Committee on Powder Diffraction Standards (JCPDS no. 82-1690). These results aligned with the findings of Lanzón *et al.*,[18] who identified calcite ($CaCO_3$) as the predominant phase in eggshell waste.

Following calcination at 700 °C, the eggshell waste appeared dark, indicating partial thermal decomposition and the presence of residual organic matter. At 800 °C, the sample appeared as a mixture of dark and white regions, suggesting further decomposition of $CaCO_3$ while still retaining a large amount of calcite. The major crystalline phase in the 700 °C and 800 °C samples was identified as calcite. At 900 °C, the eggshell waste appeared completely white, signifying full thermal decomposition. The XRD pattern of the 900 °C calcined sample displayed characteristic peaks at $2\theta = 32.20°$, 37.34°, and 53.85°, corresponding to calcium oxide (CaO) based on JCPDS no. 37-1497. This indicated that $CaCO_3$ was almost completely converted to CaO after calcination at 900 °C for 2 hours, in accordance with the thermal decomposition reaction presented in eqn (1).

$$CaCO_3\ (s) \rightarrow CaO\ (s) + CO_2\ (g) \qquad (1)$$

These findings agree with Khan *et al.*[20] and Chen *et al.*,[30] who reported that the decomposition of $CaCO_3$ occurred at temperatures above 850 °C, leading complete transformation into CaO. Furthermore, the total weight loss of the eggshell waste during calcination was 47.85%, which was closely consistent with the 46.43% weight loss reported by Chen *et al.*[30] This suggested that organic matter in the eggshell waste was fully decomposed, with carbonaceous material converted into CO_2 gas instead of remaining as char residues. Based on these results, calcination at 900 °C for 2 hours was selected as the optimal condition for further synthesis of CaO_2, as it ensured the complete decomposition of $CaCO_3$ into reactive CaO while minimizing residual organic impurities.

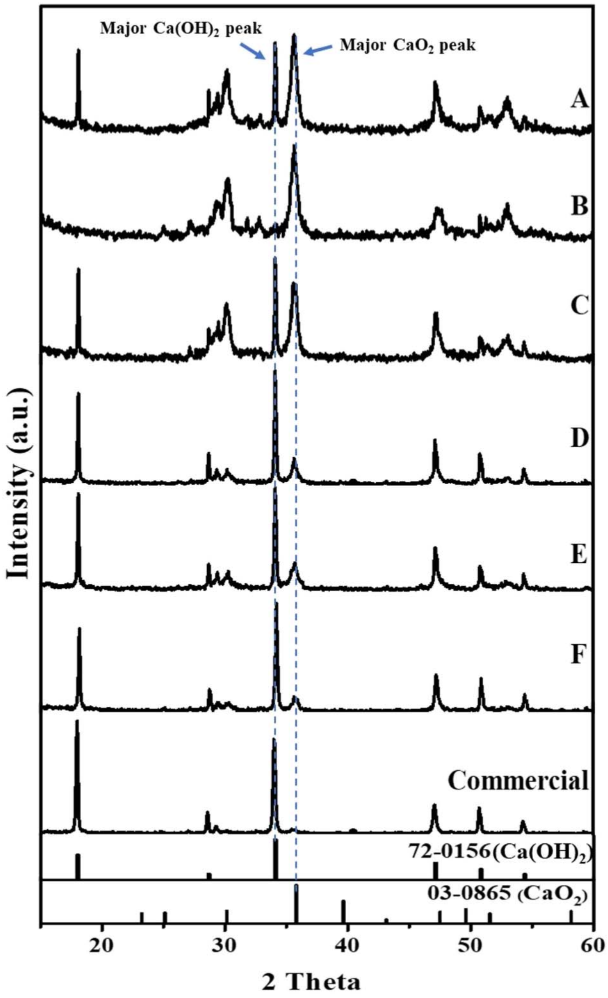

Fig. 4 XRD patterns of synthesized CaO_2 composites at different H_2O_2 concentrations. A (H_2O_2 25%, mole ratio 1 : 1), B (H_2O_2 30%, mole ratio 1 : 1), C (H_2O_2 35%, mole ratio 1 : 1), D (H_2O_2 25%, mole ratio 7 : 1), E (H_2O_2 30%, mole ratio 8.5 : 1), F (H_2O_2 35%, mole ratio 10 : 1).

As shown in Fig. 4, the XRD pattern of synthesized CaO_2 for composite B had characteristic peaks at $2\theta = 30.27°$, 35.59°, and 47.30°, which matches well with the reference pattern for CaO_2 (JCPDS no. 03-0865). In contrast, the XRD patterns of other samples showed a mixture of both the CaO_2 and $Ca(OH)_2$ phases, indicating incomplete conversion of calcium hydroxide. However, the phase fraction of $Ca(OH)_2$ in commercial CaO_2 was 95.11%, while that of CaO_2 was 4.89%. The reactions involved in CaO_2 synthesis are presented in eqn (2) and (3).

$$CaO\ (s) + H_2O\ (l) \rightarrow Ca(OH)_2\ (s) \qquad (2)$$

$$Ca(OH)_2\ (s) + H_2O_2\ (aq) \rightarrow CaO_2\ (s) + 2H_2O\ (l) \qquad (3)$$

The percentage phase fraction of CaO_2 in each sample was calculated and is summarized in Table 2. Moreover, the preparation of CaO_2 from eggshell waste allows better control of the

Table 2 Phase fraction in synthesized CaO_2 composites at different H_2O_2 concentrations

			Phase fraction (%)	
Composite	Concentration of H_2O_2 (%)	Molar ratio $Ca(OH)_2 : H_2O_2$	CaO_2	$Ca(OH)_2$
A	25	1 : 1	52.00	48.00
B	30	1 : 1	84.23	15.77
C	35	1 : 1	43.26	56.74
D	25	7 : 1	19.14	80.86
E	30	8.5 : 1	21.84	78.16
F	35	10 : 1	12.70	87.30
Commercial	—	—	4.89	95.11

CaO_2 phase fraction than commercial CaO_2, leading to improved catalytic performance. This combination of sustainability, cost-effectiveness, and enhanced material properties highlights the novelty of the present work.

3.1.1.1. Effect of H_2O_2 concentration on CaO_2 formation. According to Table 2, for composites A, B, and C, where the $Ca(OH)_2 : H_2O_2$ molar ratio was fixed at 1 : 1, an increase in H_2O_2 concentration from 25% to 30% led to a rise in the CaO_2 phase fraction from 52.00% to 84.23%. However, further increasing the H_2O_2 concentration to 35% resulted in a decrease in the CaO_2 phase fraction to 43.26%. This behavior can be explained by the Lewis base nature of H_2O_2, which possesses two lone pairs of electrons on its oxygen atoms. When H_2O_2 was introduced at 25% (composite A) and 30% (composite B), lone pair electrons from H_2O_2 readily attracted H^+ from $Ca(OH)_2$, facilitating the formation of CaO_2 according to eqn (3), with water (H_2O) as a by-product, as illustrated in Fig. 5. However, at a 35% H_2O_2 concentration (composite C), the solution pH decreased considerably. The pH of the reaction mixtures decreased with increasing H_2O_2 concentration, measured as 12.2 for composite A (25% H_2O_2), 11.8 for composite B (30% H_2O_2), and 11 for composite C (35% H_2O_2). These pH values provide quantitative support for the observed decline in the CaO_2 phase fraction at higher H_2O_2 concentrations, in agreement with the chemical reasoning based on the Lewis base behavior of H_2O_2 and proton interactions. According to Hata *et al.*,[31] increasing the H_2O_2 concentration from 0.1% to 1% led to a pH drop from 12.5 to 11.6, approaching the pK_a of H_2O_2. When excessive H_2O_2 was added, the increase in H^+ ions resulted in stronger electrostatic interactions between the H^+ and the oxygen atoms of $Ca(OH)_2$, reducing the attractive force between H_2O_2 and $Ca(OH)_2$. This hindered the formation of CaO_2, leading to a lower CaO_2 phase fraction despite the higher H_2O_2 concentration.

3.1.1.2. Effect of molar ratio on CaO_2 formation. Variations in the $Ca(OH)_2 : H_2O_2$ molar ratio from 1 : 1 to 7 : 1, 8.5 : 1, and 10 : 1 affected the crystallization of CaO_2 and the phase fraction of CaO_2 and $Ca(OH)_2$, as shown in Table 2. The observed variations in the $Ca(OH)_2$ and CaO_2 phase fractions could be primarily attributed to the crystallization process and the reaction kinetics governing CaO_2 formation. The formation of CaO_2 occurred through the reaction of $Ca(OH)_2$ with H_2O_2, where an optimal balance between reactant concentrations was necessary to maximize CaO_2 yield. At a lower $Ca(OH)_2 : H_2O_2$ molar ratio (1 : 1), a higher fraction of CaO_2 was formed due to the sufficient availability of H_2O_2 to facilitate complete conversion. However, as the molar ratio increased, the amount of unreacted $Ca(OH)_2$ also rose, leading to a progressive decline in the CaO_2 phase fraction. This trend indicates that excess $Ca(OH)_2$ did not contribute to additional CaO_2 formation but instead remained as a residual phase.

Furthermore, the crystallization dynamics suggested that the solubility and reactivity of $Ca(OH)_2$ influenced its interaction with H_2O_2. Excess $Ca(OH)_2$ likely resulted in increased particle aggregation, reducing the effective surface area available for reaction. Additionally, a higher $Ca(OH)_2$ concentration may have shifted the reaction equilibrium, hindering the complete transformation into CaO_2. These findings align with previous studies on CaO_2 synthesis mechanisms, emphasizing the importance of precise reactant ratio control to optimize phase purity and yield.[31,32]

3.1.2. Fourier-transform infrared spectroscopy analysis. FTIR analysis was performed to identify the functional groups

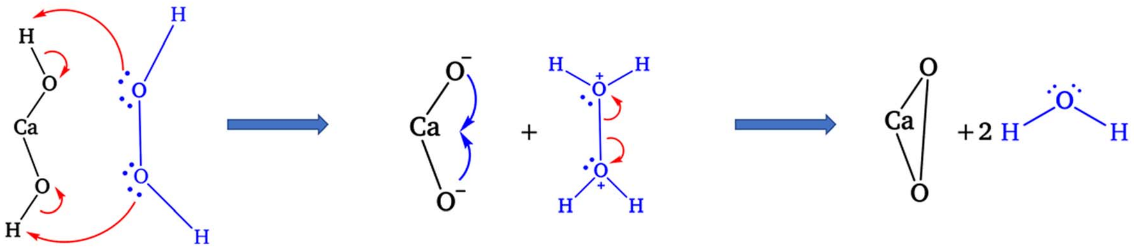

Fig. 5 Proposed mechanism of CaO_2 synthesis derived from H_2O_2 and $Ca(OH)_2$.

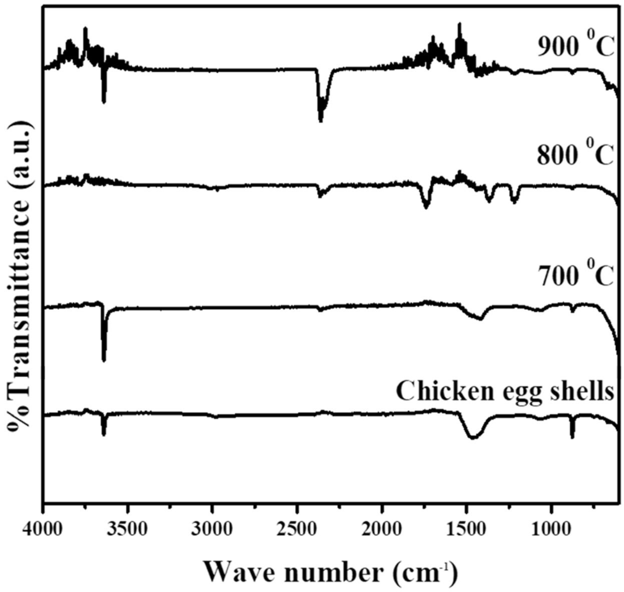

Fig. 6 Fourier-transform infrared spectroscopy spectra of eggshell waste and calcined eggshell waste at different temperatures.

present in the eggshell waste, calcined eggshell waste, and synthesized CaO_2, as shown in Fig. 6. For the eggshell waste, the FTIR spectrum confirmed characteristic carbonate (CO_3^{2-}) functional groups. The absorption band at 870 cm^{-1} corresponded to out-of-plane bending vibrations of CO_3^{2-}, while the band at 1400 cm^{-1} was attributed to asymmetric stretching vibrations of CO_3^{2-}, consistent with the findings reported by Lanzón *et al.*[18] Upon increasing the calcination temperature to 700 °C and 800 °C, the intensity of the CO_3^{2-} bands decreased, indicating partial decomposition of $CaCO_3$ into CaO. At 900 °C, the carbonate peaks were nearly absent, suggesting that most of the $CaCO_3$ had decomposed into CaO, with only minor spectral noise remaining. The absorption band at 3645 cm^{-1} was associated with the presence of hydroxyl (OH) groups, indicating surface hydration of the calcined samples.

For the synthesized CaO_2, as shown in Fig. 7, the FTIR spectrum showed characteristic O–Ca–O vibrations at 1482 cm^{-1} and 1415 cm^{-1}, while the O–O bond of the CaO_2 molecule was detected at 866 cm^{-1}.[34] These peaks closely matched the spectral features of commercial CaO_2, including the O–O vibration at 871 cm^{-1} and the O–Ca–O stretching at 1414.8 cm^{-1}, confirming the successful synthesis of CaO_2. The broad peak at 3645 cm^{-1} was attributed to hydroxyl groups, likely from surface hydration.

Moreover, the gradual loss of CO_3^{2-} bands with increasing calcination temperature indicates the thermal decomposition of $CaCO_3$ to CaO. The formation of O–Ca–O vibrations in the synthesized CaO_2 confirms the peroxide structure, while the O–O vibration at 866 cm^{-1} verifies successful incorporation of the peroxide bond. The broad band at 3645 cm^{-1} in both calcined eggshell and CaO_2 samples is attributed to surface-adsorbed water. Overall, the FTIR spectra confirm that thermal treatment and synthesis effectively converted eggshell waste into functional CaO_2 with characteristic chemical bonds.

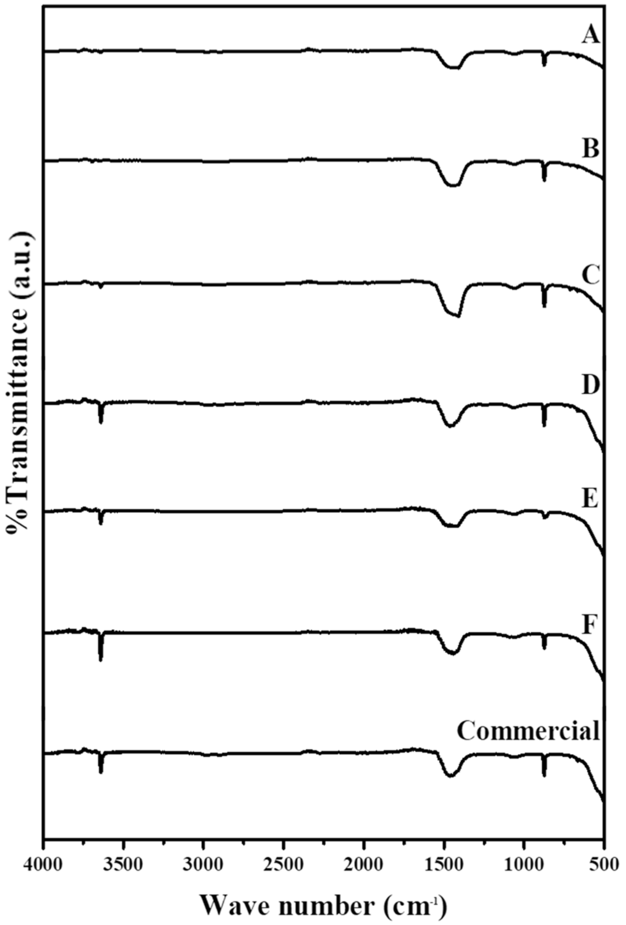

Fig. 7 Fourier-transform infrared spectroscopy spectra of synthesized CaO_2 composites (see Table 1) at different H_2O_2 concentrations: A (H_2O_2 25%, mole ratio 1 : 1), B (H_2O_2 30%, mole ratio 1 : 1), C (H_2O_2 35%, mole ratio 1 : 1), D (H_2O_2 25%, mole ratio 7 : 1), E (H_2O_2 30%, mole ratio 8.5 : 1), F (H_2O_2 35%, mole ratio 10 : 1).

3.1.3. Scanning electron microscopy analysis.

The SEM micrographs provided insights into the morphological transformations of the eggshell waste before and after calcination at different temperatures, as illustrated in Fig. 8. The SEM images of the raw eggshell waste revealed a relatively flat and compact surface morphology. However, after calcination at 900 °C, the surface became much more fragmented and porous, a transformation attributed to the thermal decomposition of calcium carbonate ($CaCO_3$) and the subsequent release of carbon dioxide (CO_2). This structural transformation resulted in a significant reduction in particle size and an increase in pore volume, thereby enhancing the specific surface area and reactivity of the materials.

Fig. 9 presents the SEM images of the synthesized CaO_2 composites obtained at different H_2O_2 concentrations. The SEM analysis confirmed the successful formation of CaO_2 particles through the reaction of $Ca(OH)_2$ with H_2O_2. However, notable agglomeration of CaO_2 particles was observed, which was likely due to the inherently high surface energy of CaO_2 particles.[20] This agglomeration phenomenon may have important implications

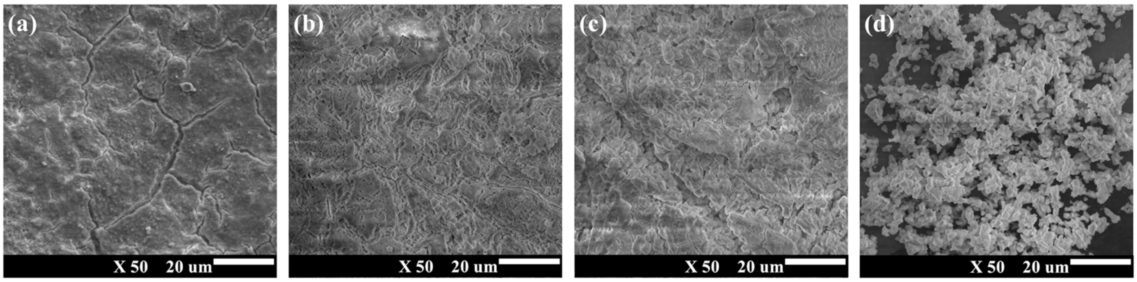

Fig. 8 Scanning electron microscopy images of eggshell waste calcined at different temperatures (a) eggshell waste, (b) 700 °C, (c) 800 °C, and (d) 900 °C.

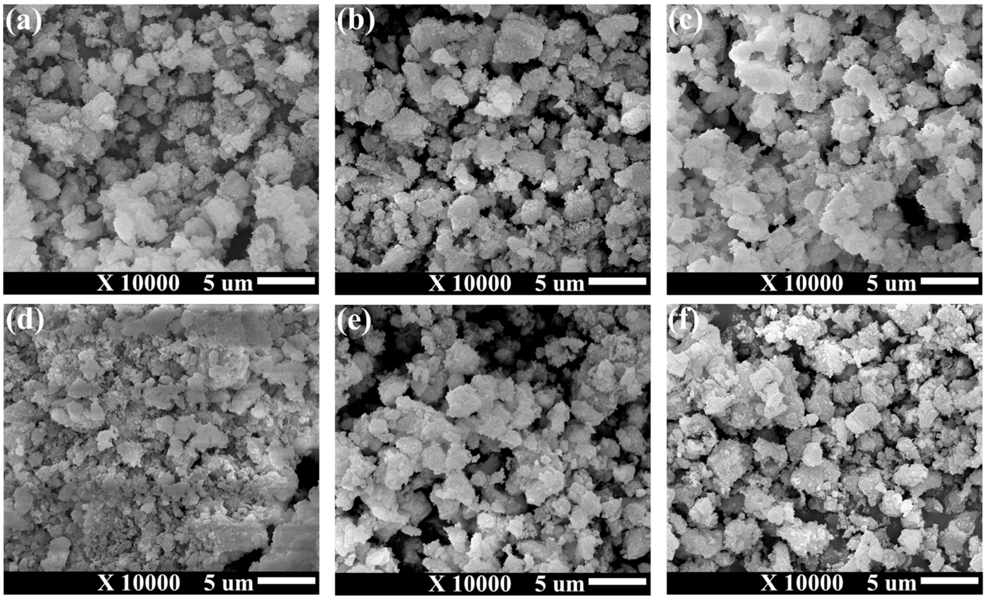

Fig. 9 Scanning electron microscopy images of synthesized CaO_2 under varying synthesis conditions, defined in Table 1 (a) composite A, (b) composite B, (c) composite C, (d) composite D, (e) composite E, and (f) composite F.

for catalytic performance, stability, and the controlled-release properties of CaO_2 in further practical applications.

3.2. Study of oxytetracycline degradation efficiency and reaction kinetic

A series of ozonation experiments were conducted at pH 7 to evaluate the efficacy of synthesized CaO_2 as a catalyst in catalytic ozonation for the degradation of OTC. Each synthesized CaO_2 composite (A–F) was applied at a dosage of 3 g L^{-1}, and the reaction was monitored at various retention times (0, 5, 10, 15, 30, and 60 min). The performance in OTC degradation was monitored and the kinetic data of catalytic ozonation were compared with sole ozonation. Based on the results (Table 3), combining the synthesized CaO_2 composites using ozonation considerably enhanced OTC removal efficiency, achieving up to 100%, compared to sole ozonation (85.72%). To our knowledge, catalytic ozonation using waste-derived CaO_2 has not been reported. In this study, CaO_2 synthesized from eggshell waste achieved complete OTC removal (100%), compared to 91.5% degradation reported by Li *et al.*[35] using commercial CaO_2 with O_3 after 30 min. In particular, composite B, which contained a higher percentage of CaO_2, showed superior OTC degradation efficiency. In contrast, composite D had a lower removal efficiency (87.86%) than the others due to its lower CaO_2 fraction. This finding confirmed the major role of CaO_2 in enhancing OTC degradation during catalytic ozonation by generating $OH^{\bullet}$ radicals that had a higher oxidation potential than ozone. These results were consistent with the findings by Giler-Molina *et al.*,[27] who reported the catalytic effectiveness of CaO_2 in advanced oxidation processes.

Based on the kinetic study, the reaction of OTC degradation by both catalytic ozonation and sole ozonation fit well with a pseudo-first-order kinetic model. According to Table 3, the observed rate constant (k_{obs}) for sole ozonation was 0.0365 $\min^{-1}$. In contrast, the k_{obs} values for catalytic ozonation using CaO_2 composites were consistently higher than for sole ozonation, indicating that the CaO_2 synthesized from the eggshell waste had considerable catalytic potential in ozonation. This enhancement in degradation efficiency could be attributed to the increased production of hydroxyl radicals

Table 3 Pseudo-first-order rate constants (k_{obs}) for oxytetracycline degradation using different synthesized CaO_2 samples at pH 7 (catalyst dosage = 3 g L^{-1})[a]

Sample	% removal at 60 min	k_{obs} (min^{-1})	R^2
Sole ozonation	85.72	0.0365	0.9820
A	100.00	0.0421	0.9666
B	100.00	0.1152	0.9142
C	100.00	0.0605	0.9782
D	100.00	0.0371	0.9928
E	100.00	0.0796	0.9536
F	87.86	0.0493	0.9776

[a] R^2 = coefficient of determination. See Table 1 for details of components of composites A–F.

($OH^{\bullet}$), which have a higher oxidation potential (2.80 V) than ozone alone (2.07 V). Among the synthesized CaO_2 composites, composite B had the highest k_{obs} value (0.1152 min^{-1}), surpassing all other composites. This superior catalytic performance could be attributed to the higher CaO_2 phase fraction in composite B, which facilitated more efficient $OH^{\bullet}$ generation, thereby accelerating OTC degradation.

At pH 7, ozone reacts *via* two primary pathways: (1) direct oxidation, in which ozone itself degrades OTC; and (2) indirect oxidation, where ozone is decomposed to generate hydroxyl radicals ($OH^{\bullet}$), which initiate secondary oxidation reactions. The presence of CaO_2 enhances $OH^{\bullet}$ generation *via* a series of mechanisms. CaO_2 slowly releases H_2O_2 and O_2, as shown in eqn (4) and (5).

$$CaO_2 + 2H_2O \rightarrow H_2O_2 + Ca(OH)_2 \quad (4)$$

$$2H_2O_2 \rightarrow 2H_2O + O_2 \quad (5)$$

Then, the hydroxyl radical ($OH^{\bullet}$) is generated through the reaction between H_2O_2 and O_3, as shown in eqn (6)–(10).

$$H_2O_2 + H_2O \rightarrow HO_2^- + H_3O^+ \quad (6)$$

$$O_3 + HO_2^- \rightarrow HO_2^- + O_2 \quad (7)$$

$$O_3 + HO_2^- \rightarrow OH^{\bullet} + O_2^- + O_2 \quad (8)$$

$$O_3 + O_2^- \rightarrow O_3^- + O_2 \quad (9)$$

$$O_3^- + H_2O \rightarrow OH^{\bullet} + O_2 + OH^- \quad (10)$$

Furthermore, the dissociation of $Ca(OH)_2$ releases OH^- ions, leading to an increase in pH, which in turn promotes the formation of hydroperoxyl radicals ($HO_2^{\bullet}$), as illustrated in eqn (11) and (12).[6,8,33]

$$Ca(OH)_2 \rightarrow Ca^{2+} + 2OH^- \quad (11)$$

$$OH^- + O_3 \rightarrow HO_2^{\bullet} + O_2 \quad (12)$$

These findings suggest that the CaO_2 synthesized from eggshell waste not only serves as an efficient catalyst for OTC degradation *via* ozonation but also provides a promising and sustainable alternative to commercial CaO_2 catalysts.

4. Conclusions

CaO_2 was successfully synthesized from eggshell waste and its effectiveness was demonstrated as a catalyst in the ozonation process for the degradation of oxytetracycline (OTC). The optimal calcination temperature was 900 °C for converting $CaCO_3$ from the eggshell waste into CaO, ensuring complete phase transformation. For CaO_2 synthesis, the optimum $Ca(OH)_2$-to-H_2O_2 molar ratio was 1 : 1, with an H_2O_2 concentration of 30%, yielding the highest CaO_2 phase fraction (84.23%). The synthesized CaO_2 composites combined with ozonation considerably enhanced OTC degradation efficiency, achieving up to 100% removal, compared to sole ozonation (85.72%).

Based on the kinetic analysis, the value of the pseudo-first-order rate constant (k_{obs}) was 0.1152 min^{-1}, for catalytic ozonation using composite B as a catalyst, which was considerably higher than that of sole ozonation (0.0365 min^{-1}) and even greater than that of commercial CaO_2 (0.0880 min^{-1}). This enhanced oxidation performance was primarily attributed to the higher CaO_2 phase fraction in composite B, which facilitated efficient generation of hydroxyl radicals ($OH^{\bullet}$), providing a higher oxidative potential.

In summary, CaO_2 synthesized from eggshell waste with a high fraction of CaO_2 demonstrates significant potential as an effective catalyst for catalytic ozonation processes. This study highlighted the feasibility of using waste-derived CaO_2 as a sustainable and efficient catalyst for advanced oxidation processes.

Author contributions

Apiradee Sukmilin: conceptualization; data curation; formal analysis; funding acquisition; project administration; writing – original draft and manuscript editing. Piyapong Pankaew: data curation; XRD, SEM and FTIR analysis; characterization; writing. Jaroenporn Chokboribal: FTIR analysis and graphical drawing. Chalor Jarusutthirak: conceptualization and manuscript editing.

Conflicts of interest

The authors declare that they have no known competing financial interests or personal relationships that could have appeared to influence the work reported in this paper.

Data availability

Data underlying this study are available from the corresponding author on reasonable request.

Acknowledgements

This work (Grant No. RGNS 65-166) was financially supported by Office of the Permanent Secretary, Ministry of Higher Education, Science, Research and Innovation (OPSMHESI), by the Thailand Science Research and Innovation (TSRI), and by Phranakhon Rajabhat University.

References

1 H. Wang, Y. Zhao, T. Li, Z. Chen, Y. Wang and C. Qin, Properties of calcium peroxide for release of hydrogen peroxide and oxygen: a kinetic study, *J. Chem. Eng.*, 2016, **303**, 450–457, DOI: **10.1016/j.cej.2016.05.123**.

2 S. Lu, X. Zhang and Y. Xue, Application of calcium peroxide in water and soil treatment: a review, *J. Hazard. Mater.*, 2017, **337**, 163–177, DOI: **10.1016/j.jhazmat.2017.04.064**.

3 Q. Xu, Q.-S. Huang, W. Wei, J. Sun, X. Dai and B.-J. Ni, Improving the treatment of waste activated sludge using calcium peroxide, *Water Res.*, 2020, **187**, 116440, DOI: **10.1016/j.watres.2020.116440**.

4 Z. Honarmandrad, N. Javid and M. Malakootian, Efficiency of ozonation process with calcium peroxide in removing heavy metals (Pb, Cu, Zn, Ni, Cd) from aqueous solution, *SN Appl. Sci.*, 2020, **2**, 703, DOI: **10.1007/s42452-020-2392-1**.

5 H.-B. Kim, J.-G. Kim, D. S. Alessi and K. Baek, Mitigation of arsenic release by calcium peroxide (CaO_2) and rice straw biochar in paddy soil, *Chemosphere*, 2023, **324**, 138321, DOI: **10.1016/j.chemosphere.2023.138321**.

6 B. Balci, F. E. Erkurt, F. Budak, Z. Zaimoglu, M. Basibuyuk and H. K. Yesiltas, Degradation of a basic textile dye by inactivated calcium peroxide, *Desalin. Water Treat.*, 2022, **258**, 111–122, DOI: **10.5004/dwt.2022.28419**.

7 B. Balci, N. Aksoy, F. E. Erkurt, F. Budak, M. Basibuyuk, Z. Zaimoglu, E. S. Turan and S. Yilmaz, Removal of a reactive dye from simulated textile wastewater by environmentally friendly oxidant calcium peroxide, *Int. J. Chem. React. Eng.*, 2021, 62, DOI: **10.1515/ijcre-2021-0062**.

8 Z. Honarmandrad, N. Javid and M. Malakootian, Removal efficiency of phenol by ozonation process with calcium peroxide from aqueous solutions, *Appl. Water Sci.*, 2021, **11**, 14, DOI: **10.1007/s13201-020-01344-7**.

9 H. N. P. Vo, H. H. Ngo, W. Guo, K. H. Nguyen, S. W. Chang, D. D. Nguyen, D. Cheng, X. T. Bui, Y. Liu and X. Zhang, Effect of calcium peroxide pretreatment on the remediation of sulfonamide antibiotics (SMs) by *Chlorella* sp, *Sci. Total Environ.*, 2021, **793**, 148598, DOI: **10.1016/j.scitotenv.2021.148598**.

10 Z. Honarmandrad, A. Asadipour and M. Malakootian, Investigating the use of ozonation process with calcium peroxide for the removal of metronidazole antibiotic from aqueous solutions, *Desalin. Water Treat.*, 2017, **77**, 315–320, DOI: **10.5004/dwt.2017.20764**.

11 L. Xiang, Z. Xie, H. Guo, J. Song, D. Li, Y. Wang, S. Pan, S. Lin, Z. Li, J.-G. Han and W. Qiao, Efficient removal of emerging contaminant sulfamethoxazole in water by ozone coupled with calcium peroxide: mechanism and toxicity assessment, *Chemosphere*, 2021, **283**, 131156, DOI: **10.1016/j.chemosphere.2021.131156**.

12 X. Wang, L. Zhang, C. Han, Y. Zhang and J. Zhuo, Simulation study of oxytetracycline contamination remediation in groundwater circulation wells enhanced by nano-calcium peroxide and ozone, *Sci. Rep.*, 2023, **13**(1), 9136, DOI: **10.1038/s41598-023-36310-1**.

13 M. Izadifard, G. Achari and C. H. Langford, Mineralization of sulfolane in aqueous solutions by ozone/CaO_2 and ozone/CaO with potential for field application, *Chemosphere*, 2018, **197**, 535–540, DOI: **10.1016/j.chemosphere.2018.01.072**.

14 P. Chookaew, A. Sukmilin and C. Jarusutthirak, Optimization of diclofenac treatment in synthetic wastewater using catalytic ozonation with calcium peroxide as catalyst, *Environ. Nat. Resour. J.*, 2024, **22**(4), 354–365, DOI: **10.32526/ennrj/22/20240102**.

15 J. Khoddaveisi, H. Banejad, A. Afkhami, E. Olyaie, S. Lashgari and R. Dashti, Synthesis of calcium peroxide nanoparticles as an innovative reagent for in situ chemical oxidation, *J. Hazard. Mater.*, 2011, **192**(3), 1437–1440, DOI: **10.1016/j.jhazmat.2011.06.060**.

16 P. Kaewdee, N. Chandet, G. Rujijanagul and C. Randorn, Multicatalytic properties of nanoparticle CaO_2 synthesized by a novel, simple and economical method for wastewater treatment, *Catal. Commun.*, 2016, **84**, 151–154, DOI: **10.1016/j.catcom.2016.06.031**.

17 P. Vijuksungsith, T. Satapanajaru, C. Chokejaroenrat, C. Jarusutthirak, C. Sukulthaew, A. Kambhu and R. Boonprasert, Remediating oxytetracycline-contaminated aquaculture water using nano calcium peroxide ($nCaO_2$) produced from flue gas desulfurization (FDG) gypsum, *Environ. Technol. Innovation*, 2021, 24101861, DOI: **10.1016/j.eti.2021.101861**.

18 M. Lanzón, J. A. Madrid-Mendoza, D. Navarro-Moreno and V. E. García-Vera, Use of eggshell waste: a green and effective method for the synthesis of pure calcium hydroxide suspensions, *Constr. Build. Mater.*, 2023, **367**, 131106, DOI: **10.1016/j.conbuildmat.2023.131106**.

19 V. Vandeginste, Food waste eggshell valorization through development of new composites: a review, *Sustainable Mater. Technol.*, 2021, **29**, e00317, DOI: **10.1016/j.susmat.2021.e00317**.

20 S. R. Khan, S. Jamil, H. Rashid, R. Ali and S. A. Khan, Agar and egg shell derived calcium carbonate and calcium hydroxide nanoparticles: synthesis, characterization and applications, *Chem. Phys. Lett.*, 2019, **732**, 136662, DOI: **10.1016/j.cplett.2019.136662**.

21 W. Heo, H. Shin, J. R. Ansari, K. Park and J. Seo, Preparation and properties of calcium oxide and calcium peroxide from eggshell waste for enhanced antimicrobial activity, *Mater. Today Commun.*, 2024, **41**, 110531, DOI: **10.1016/j.mtcomm.2024.110531**.

22 A. Rastinfard, M. H. Nazarpak and F. Moztarzadeh, Controlled chemical synthesis of CaO_2 particles coated with polyethylene glycol: characterization of crystallite size

and oxygen release kinetics, *RSC Adv.*, 2018, **8**, 91, DOI: 10.1039/c7ra08758f.

23 Z. Maghsodian, A. M. Sanati, T. Mashifana, M. Sillanpää, S. Feng, T. Nhat and B. Ramavandi, Occurrence and distribution of antibiotics in the water, sediment, and biota of freshwater and marine environments: a review, *Antibiotics*, 2022, **11**, 1461, DOI: 10.3390/antibiotics11111461.

24 A. Rico, R. Oliverira, S. McDonough, A. Matser, J. Khatikarn, K. Satapornvanit, A. J. A. Nogueira, A. M. V. M. Soares, I. Domingues and P. J. van den Brink, Use, fate and ecological risks of antibiotics applied in tilapia cage farming in Thailand, *Environ. Pollut.*, 2014, **191**, 8–16, DOI: 10.1016/j.envpol.2014.04.002.

25 J.-A. Park, M. Pineda, M.-L. Peyot and V. Yargeau, Degradation of oxytetracycline and doxycycline by ozonation: degradation pathways and toxicity assessment, *Sci. Total Environ.*, 2023, **856**(1), 159076, DOI: 10.1016/j.scitotenv.2022.159076.

26 K. Li, A. Yeddiler, M. Yang, S. Schulte-Hostede and M. H. Wong, Ozonation of oxytetracycline and toxicological assessment of its oxidation by products, *Chemosphere*, 2008, **73**, 473–478, DOI: 10.1016/j.chemosphere.2008.02.008.

27 J. M. Giler-Molina, L. A. Zambrano-Intriago, L. S. Quiroz-Fernandez, D. C. Napoleao, J. S. Vieira, N. S. Oliverira and J. M. Rodriguez-Diaz, Degradation of oxytetracycline in aqueous solutions: application of homogeneous and heterogenous advanced oxidation processes, *Sustainability*, 2022, **12**, 8807, DOI: 10.3390/su12218807.

28 Z. Chen, P. Ju, S. Lu, G. Zhang, Y. Chen, Z. Zhu and F. Jiang, Waste to worth: facile preparation of CaO_2 derived from oyster shells for highly efficient degradation of organic contaminants based on Fenton-like system, *Inorg. Chem. Commun.*, 2024, **16**, 112378, DOI: 10.1016/j.inoche.2024.112378.

29 Y. M. Sung, J. U. Lee and J. W. Yang, Crystallization and sintering characteristics of chemically precipitated hydroxyapatite nanopowder, *J. Cryst. Growth*, 2004, **262**, 467–472, DOI: 10.1016/j.jcrysgro.2003.10.001.

30 W. Chen, Y. Wu, Z. Xie, Y. Li, W. Tang and J. Yu, Calcium hydroxide recycled from waste eggshell resources for the effective recovery of fluoride from wastewater, *RSC Adv.*, 2022, **12**, 282264–28278, DOI: 10.1039/d2ra05209a.

31 Y. Hata, Y. Bouda, S. Hiruma, H. Miyazaki and S. Nakamura, Biofilm degradation by seashell-derived calcium hydroxide and hydrogen peroxide, *Nanomater*, 2022, **12**(20), 3681, DOI: 10.3390/nano12203681.

32 S. Shen, M. Mamat, S. Zhang, J. Cao, Z. D. Hood, L. Figueroa-Cosme and Y. Xia, Synthesis of CaO_2 nanocrystals and their spherical aggregates with uniform sizes for use as a biodegradable bacteriostatic agent, *Small*, 2019, **15**(36), e1902118, DOI: 10.1002/smll.201902118.

33 M. K. Mohsin and A. A. Mohammed, Catalytic ozonation for removal of antibiotic oxy-tetracycline using zinc oxide nanoparticles, *Appl. Water Sci.*, 2021, **11**(9), 1–9, DOI: 10.1007/s13201-020-01333-w.

34 B. S. De, K. L. Wasewar, V. R. Dhongde, S. S. Madan and A. V. Gomase, Recovery of Acrylic Acid Using Calcium Peroxide Nanoparticles: Synthesis, Characterisation, Batch Study, Equilibrium, and Kinetics, *Chem. Biochem. Eng. Q.*, 2018, **32**(1), 29–39, DOI: 10.15255/CABEQ.2016.1055b.

35 Z. Li, L. Xiang, S. Pan, D. Zhu, S. Li and H. Guo, The Degradation of Aqueous Oxytetracycline by an O_3/CaO_2 System in the Presence of HCO^{-3}: Performance, Mechanism, Degradation Pathways, and Toxicity Evaluation, *MOLEFW.*, 2024, **29**(659), 1–19, DOI: 10.3390/molecules29030659.